Bumps, breathers, and waves in a neural network with spike frequency adaptation

S. Coombes and M.R. Owen

School of Mathematical Sciences, University of Nottingham, Nottingham, NG7 2RD, UK
(Dated: March 2, 2005)

In this Letter we introduce a continuum model of neural tissue that include the effects of so-called spike frequency adaptation (SFA). The basic model is an integral equation for synaptic activity that depends upon the non-local network connectivity, synaptic response, and firing rate of a single neuron. A phenomenological model of SFA is examined whereby the firing rate is taken to be a simple state-dependent threshold function. As in the case without SFA classical Mexican-Hat connectivity is shown to allow for the existence of spatially localized states (bumps). Importantly an analysis of bump stability using recent Evans function techniques shows that bumps may undergo instabilities leading to the emergence of both breathers and traveling waves. Moreover, a similar analysis for traveling pulses leads to the conditions necessary to observe a stable traveling breather. Direct numerical simulations both confirm our theoretical predictions and illustrate the rich dynamic behavior of this model, including the appearance of self-replicating bumps.

Neural field models of Wilson-Cowan [1] or Amari [2] type have been intensively studied since the 1970's with regard to the dynamics of large scale brain activity. This has had a major impact in helping not only to understand the dynamics seen in brain slice preparations [3], but also in understanding EEG rhythms [4], visual hallucinations [5, 6], short term memory [7], motion perception [8], representations in the head-direction system [9] and feature selectivity in the visual cortex [10]. For a recent review of the dynamics of neural fields we refer the reader to [11]. Typically, however, such models do not incorporate any of the slow intrinsic processes known to modulate single neuron response. In this Letter we focus on the effects of one such process, namely spike frequency adaptation (SFA). SFA is a commonly observed property of many single neurons and has been linked to the presence of a Ca^{2+} gated K^+ current, I_{AHP} [12]. The generation of an action potential leads to a small calcium influx that increments I_{AHP}, with the end result being a decrease in the firing rate response to persistent stimuli. Both biophysical and phenomenological models of this process have been studied in the context of neural computation at the single cell level (see for example the work of Liu and Wang [13]). In this Letter we show that SFA can also lead to novel dynamic instabilities at the network level. To illustrate this we focus on a one-dimensional neural field model with short-range excitation and long range inhibition, and consider a simple model of SFA.

In more detail we analyze a neural field model with synaptic activity $u = u(x,t)$, $x \in \mathbb{R}$, $t \in \mathbb{R}^+$, governed by the integral equation

$$u = \eta * w \otimes H(u - h). \qquad (1)$$

Here, the symbol $*$ represents a temporal convolution in the sense that

$$(\eta * f)(x,t) = \int_0^t \eta(s)f(x,t-s)\mathrm{d}s, \qquad (2)$$

and $\otimes$ represents a spatial convolution such that

$$(w \otimes f)(x,t) = \int_{-\infty}^{\infty} w(y)f(x-y,t)\mathrm{d}y. \qquad (3)$$

The function $\eta(t)$ (with $\eta(t) = 0$ for $t < 0$) represents a synaptic filter, whilst $w(x)$ is a synaptic footprint describing the anatomy of network connections. The function H represents the firing rate of a single neuron, and we shall take it to be a Heaviside function such that $H(x) = 1$ for $x \geq 0$ and is zero otherwise. Hence, we identify h as a firing threshold. In the absence of an SFA current we would recover the standard model (without SFA), by setting h to be a constant, say h_0. To mimic the effects of SFA we consider an adaptive threshold that changes most when synaptic input to a neuron is large. One such simple adaptive scheme, in the spirit of that discussed in [13], can be written

$$h_t = -(h - h_0) + \kappa H(u - \theta), \qquad (4)$$

for some SFA threshold θ and positive κ. In fact a linear threshold dynamics has previously been considered in [10], and can be traced all the way back to work by Hill in 1936 [14]. However, the form of *nonlinear* threshold dynamics chosen here leads to interesting new phenomena. For the rest of this paper we work with the choice $\eta(t) = \alpha e^{-\alpha t}H(t)$ and $w(x) = (1-|x|)e^{-|x|}$. The extension to other synaptic filters and footprints is straightforward [15].

First we construct time-independent solutions $(u,h) = (q(x), p(x))$ that satisfy

$$q = w \otimes H(q-p), \qquad p = \begin{cases} h_0 & q < \theta \\ h_0 + \kappa & q \geq \theta \end{cases}. \qquad (5)$$

A localized bump solution is one that satisfies $q(x) > h_0 + \kappa$ for $x \in [0, x_1]$, $\theta < q(x) < h_0 + \kappa$ for $x \in (x_1, x_2)$,
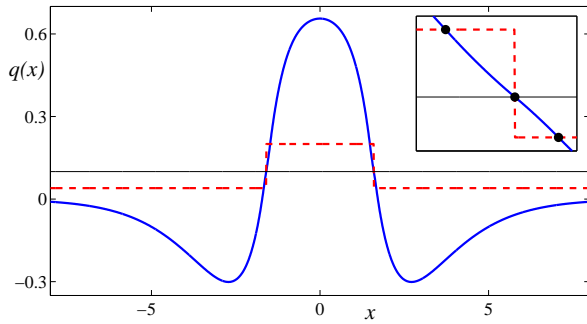
FIG. 1: (Color online). Analytical bump solution (q, p) (as solid and dashed lines respectively) with $h_0 = 0.04$ $\theta = 0.1$, $\kappa = 0.16$. Here $x_1 = 1.48$, $x_2 = 1.60$ and $x_3 = 1.67$. The inset shows a blowup of the solution around the window containing the points x_1, x_2 and x_3. At these parameter values this type of solution exits for $\kappa < 0.32$.

$h_0 < q(x) \leq \theta$ for $x \in [x_2, x_3]$ and $q(x) < h_0$ otherwise. Furthermore, we restrict attention to symmetric solutions for which $q(x) = q(-x)$ with $x_3 > x_2 > x_1 > 0$. An explicit solution may be constructed as

$$q(x) = \left(\int_{-x_3}^{-x_2} + \int_{-x_1}^{x_1} + \int_{x_2}^{x_3} \right) w(x - y) \mathrm{d}y. \quad (6)$$

The unknowns x_1, x_2, and x_3 are found by the simultaneous solution of

$$q(x_1) = h_0 + \kappa, \quad q(x_2) = \theta, \quad q(x_3) = h_0. \quad (7)$$

A plot of an analytical bump solution constructed in this fashion is shown in Fig. 1. It appears that for κ less than some critical value there is only ever one solution of this type. To assess the linear stability of this solution we study perturbations of the form $u(x, t) = q(x) + \delta u(x, t)$, and $h(x, t) = p(x) + \delta h(x, t)$. An expansion of (1) and (4) and working to first order generates the pair of equations

$$\delta u = \eta * w \otimes H'(q - p)[\delta u - \delta h], \quad (8)$$
$$\delta h = \eta_h * \kappa H'(q - \theta)\delta u, \quad (9)$$

where $\eta_h(t) = \mathrm{e}^{-t} H(t)$. Here H' is the derivative of H, i.e. $H'(x) = \delta(x)$. For perturbations of the form $(\delta u(x, t), \delta h(x, t)) = (u(x), h(x))\mathrm{e}^{\lambda t}$ we have that

$$\frac{u}{\mathcal{L}[\eta](\lambda)} = w \otimes H'(q - p) \left[1 - \kappa \mathcal{L}[\eta_h](\lambda) H'(q - \theta) \right] u, \quad (10)$$

where we have eliminated the equation for h using (9) and introduced the Laplace transform $\mathcal{L}[\eta](\lambda) = \int_0^\infty \mathrm{d}s e^{-\lambda s} \eta(s)$. Making use of the fact that

$$\delta(q(x) - p(x)) = \sum_{y = \pm x_1, \pm x_3} \frac{\delta(x - y)}{|q'(q^{-1}(y))|}, \quad (11)$$

and

$$\delta(q(x) - p(x))\delta(q(x) - \theta) = \frac{1}{\kappa} \sum_{y = \pm x_2} \frac{\delta(x - y)}{|q'(q^{-1}(y))|}, \quad (12)$$

means that (10) takes the form

$$\frac{u(x)}{\mathcal{L}[\eta](\lambda)} = \sum_{j=1}^{6} A_j(x, \lambda) u_j, \quad (13)$$

where $u_j = u(x_j)$ and $(x_4, x_5, x_6) = -(x_1, x_2, x_3)$, $A_1(x, \lambda) = w(x - x_1)/|q'(x_1)| = A_4(-x, \lambda)$, $A_2(x, \lambda) = -\mathcal{L}[\eta_h](\lambda) w(x - x_2)/|q'(x_2)| = A_5(-x, \lambda)$, and $A_3(x, \lambda) = w(x - x_3)/|q'(x_3)| = A_6(-x, \lambda)$. The derivative of q is easily calculated from (6) as $q'(x) = W(x) - W(-x)$, where $W(x) = w(x + x_1) - w(x + x_2) + w(x + x_3)$. Demanding that the perturbations at x_j be non-trivial generates an eigenvalue problem of the form $\mathcal{E}(\lambda) = 0$, where $\mathcal{E}(\lambda) = \left| \mathcal{L}[\eta](\lambda)^{-1} I_6 - \mathcal{A}(\lambda) \right|$, I_n is the $n \times n$ identity matrix and $\mathcal{A}(\lambda)$ has components

$$\mathcal{A}(\lambda)_{ij} = A_j(x_i, \lambda), \qquad i, j = 1, \dots, 6. \quad (14)$$

We identify $\mathcal{E}(\lambda)$ as the Evans function for the bump, such that solutions are stable if Re $\lambda < 0$. A recent discussion of the use of Evans function techniques in neural field theories can be found in [16]. Using the fact that $\mathcal{L}[\eta_h](0) = 1 = \mathcal{L}[\eta](0)$ a direct calculation shows that $\mathcal{E}(0) = 0$ (with corresponding eigenfunction $q'(x)$), as expected for a system with translation invariance. By determining the zeros of the Evans function we are now in a position to probe the manner in which a bump may go unstable. One natural way to find the zeros of $\mathcal{E}(\lambda)$ is to write $\lambda = \nu + \mathrm{i}\omega$ and plot the zero contours of Re $\mathcal{E}(\lambda)$ and Im $\mathcal{E}(\lambda)$ in the (ν, ω) plane. The Evans function is zero where the lines intersect. There are basically two different routes to instability: i) for sufficiently small κ an eigenvalue crosses to the right hand complex plane on the real axis, and one sees a bump go unstable in favor of a traveling pulse with increasing α, and ii) for larger κ a pair of complex-conjugate eigenvalues cross through the imaginary axis to the right hand complex plane and a bump goes unstable in favor of a breathing solution, with increasing α. These two scenarios are illustrated in Fig. 2 and Fig. 3 respectively.

It is possible to extend this analysis to traveling wave solutions, and in particular the type of solution shown in Fig. 2. Following the approach in [16] we introduce the coordinate $\xi = x - ct$ and seek functions $\widetilde{u}(\xi, t) = u(x - ct, t)$ and $\widetilde{h}(\xi, t) = h(x - ct, t)$ that satisfy (1) and (4). In the (ξ, t) coordinates we have that

$$\widetilde{u}(\xi, t) = \int_{-\infty}^{\infty} \mathrm{d}y w(y) \int_0^{\infty} \mathrm{d}s \eta(s)$$
$$\times H(\widetilde{u}(\xi - y + cs, t - s) - \widetilde{h}(\xi - y + cs, t - s)), \quad (15)$$

$$\widetilde{h}(\xi, t) = h_0 + \kappa \int_0^{\infty} \mathrm{d}s \eta_h(s) H(\widetilde{u}(\xi + cs, t - s) - \theta). \quad (16)$$
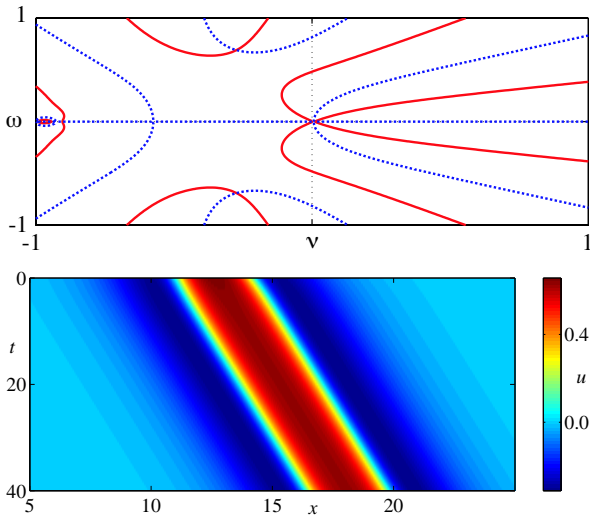
FIG. 2: (Color online). Top: A plot of the Evans function for a localized bump solution at $\kappa = 0.16$, and other parameters as in Fig. 1. Zeros of the Evans function occur at the intersection of the solid and dashed lines where $\mathrm{Re}\,\mathcal{E}(\lambda) = 0 = \mathrm{Im}\,\mathcal{E}(\lambda)$. As α increases through $\alpha_c \sim 1.55$ an eigenvalue crosses to the the right hand complex plane along the real axis, signaling the onset of an instability. Bottom: a space-time plot showing an example of a traveling pulse seen just after the point of instability.

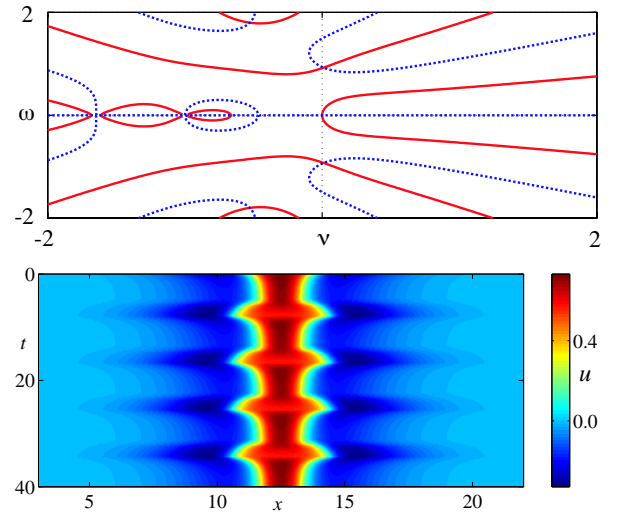FIG. 3: (Color online). Top: A plot of the Evans function for a localized bump solution at $\kappa = 0.3$, and other parameters as in Fig. 1. As α increases through $\alpha_c \sim 3.0$ an eigenvalue crosses to the the right hand complex plane through the imaginary axis, signaling the onset of a dynamic instability. Bottom: a space-time plot showing an example of a breathing solution seen just after the point of instability.

The traveling wave is a stationary solution $(\widetilde{u}(\xi,t), \widetilde{h}(\xi,t)) = (q(\xi), p(\xi))$ that satisfies

$$q(\xi) = \int_0^\infty \mathrm{d}s\, \eta(s)\psi(\xi + cs), \tag{17}$$

$$\psi(\xi) = \int_{-\infty}^\infty \mathrm{d}y\, w(y) H(q(\xi - y) - p(\xi - y)), \tag{18}$$

$$p(\xi) = h_0 + \kappa \int_0^\infty \mathrm{d}s\, \eta_h(s) H(q(\xi + cs) - \theta). \tag{19}$$

We now consider traveling pulse solutions of the form $q(\xi) \geq \theta$ for $\xi \in [\xi_1, \xi_3]$ and $q(\xi) < \theta$ otherwise. In this case the solution for $p(\xi)$ is easily calculated from (19) as

$$p(\xi) = h_0 + \kappa \begin{cases} [1 - e^{-(\xi_3 - \xi_1)/c}]e^{(\xi - \xi_1)/c} & \xi < \xi_1 \\ 1 - e^{(\xi - \xi_3)/c} & \xi_1 \leq \xi \leq \xi_3 \\ 0 & \xi > \xi_3 \end{cases} . \tag{20}$$

We further restrict our attention to traveling pulse solutions where $q(\xi) > p(\xi)$ for $\xi \in (\xi_2, \xi_4)$, and $q(\xi) < p(\xi)$ otherwise, with $\xi_1 < \xi_2 < \xi_3 < \xi_4$. In this case (18) takes the simple form

$$\psi(\xi) = \int_{\xi_2 - \xi}^{\xi_4 - \xi} \mathrm{d}y\, w(y). \tag{21}$$

Hence the solution for $q(\xi)$ is parameterised by the five unknowns $\xi_1, \xi_2, \xi_3, \xi_4, c$. By choosing an origin such that

$\xi_1 = 0$ the simultaneous solution of the four threshold crossing conditions

$$q(\xi_1) = \theta \quad q(\xi_2) = p(\xi_2) \quad q(\xi_3) = \theta \quad q(\xi_4) = p(\xi_4), \tag{22}$$

may be used to determine the remaining four unknowns. Linearising (15) and (16) about the travelling pulse and seeking solutions of the form $(u(\xi), h(\xi))e^{\lambda t}$ gives

$$u(\xi) = A_2(\xi, \lambda)[u(\xi_2) - h(\xi_2)] + A_4(\xi, \lambda)[u(\xi_4) - h(\xi_4)], \tag{23}$$

$$h(\xi) = A_1(\xi, \lambda)u(\xi_1) + A_3(\xi, \lambda)u(\xi_3), \tag{24}$$

where $A_i(\xi, \lambda) = -\mathcal{H}(\xi_i - \xi), \lambda)/|q'(\xi_i)|$ for $i = 1, 3$ and $A_i(\xi, \lambda) = \mathcal{U}(\xi_i - \xi, \lambda)/|F'(\xi_i)|$ for $i = 2, 4$. Here, $F(s) = q(s) - p(s)$ and

$$c\,\mathcal{U}(\xi, \lambda) = \int_0^\infty \mathrm{d}y\, w(y - \xi)\eta(y/c)e^{-\lambda y/c}, \tag{25}$$

$$c\,\mathcal{H}(\xi, \lambda) = \kappa \eta_h(\xi/c)e^{-\lambda \xi/c}. \tag{26}$$

The derivatives q' and p' are easily calculated as $\alpha(q - \psi)/c$ and $(p - h_0 - \kappa H(q - \theta))/c$ respectively. Following along identical lines to the construction of the Evans function for a bump we obtain $\mathcal{E}(\lambda) = |I_3 - \mathcal{A}(\lambda)| = 0$, where the 3×3 matrix $\mathcal{A}(\lambda)$ has components $[\mathcal{A}(\lambda)]_{ij} = A_j(\xi_i, \lambda)$. A straightforward calculation establishes that $(u, h) = (q', p')$ is an eigenfunction with $\lambda = 0$ as expected. Interestingly, our analysis shows that stable traveling pulses co-exist with stable bump solutions for a wide
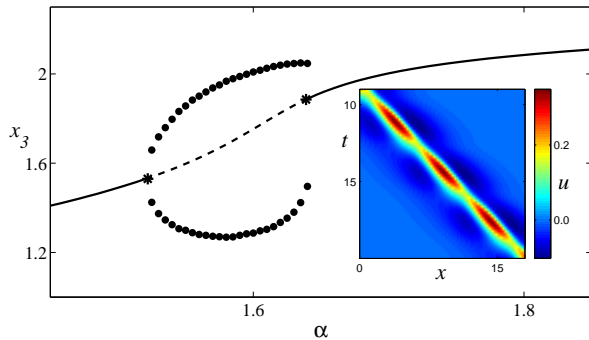
FIG. 4: (Color online). Analytically determined width x_3 of a traveling pulse solution as a function of the synaptic rate constant α (solid line is stable, dashed is unstable). As α increases through $\alpha \sim 1.52$ the Evans function shows that a pair of complex-conjugate eigenvalues crosses to the right hand complex plane. At $\alpha \sim 1.64$ they cross back to the left hand complex plane. This leads to a branch of traveling breather solutions whose width oscillates between the indicated maximum and minimum values (circles). The inset shows an example of such a traveling breather, at $\alpha = 1.58$.

range of parameter values. Moreover, it is possible that a pulse can undergo a dynamic instability with increasing α and then restabilize via the reverse mechanism. Direct numerical simulations in such parameter windows show the emergence of stable traveling breathers. We illustrate this phenomenon in Fig. 4. In fact direct numerical simu-
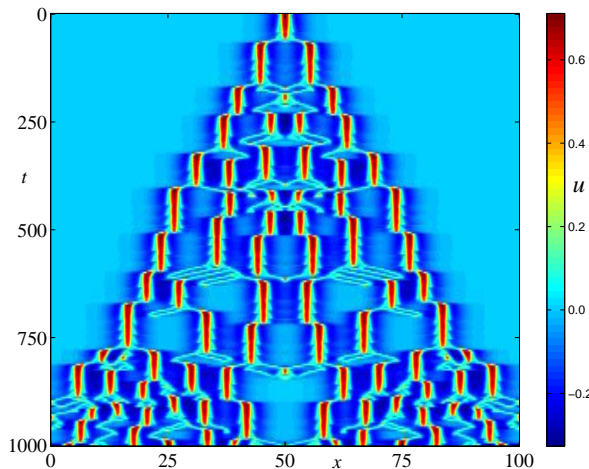

FIG. 5: (Color online). An example of a self-replicating bump in a regime where single bumps do not exist. Parameters are $h_0 = 0.02, \theta = 0.1, \kappa = 0.34$ and $\alpha = 0.5$.

lations (for Heaviside, sigmoidal and threshold linear firing rate functions) show a whole host of exotic solutions including asymmetric breathers, multiple bumps, multiple pulses, periodic traveling waves, and bump-splitting instabilities that appear to lead to spatio-temporal chaos. An example of a such a splitting is shown in Fig. 5. It is interesting to note that similar bifurcations have been seen in other dissipative systems that support localized

structures, in particular those of coupled cubic complex Ginzburg-Landau equations [17]. Moreover, the traveling pulses in our model exhibit particle like properties, and are reminiscent of the dispersive solitons observed in some three component reaction-diffusion systems [18]. Although such behavior may well be generic in inhomogeneous neural field models with external forcing, as in the work of Bressloff *et al.* [19], to our knowledge this is the first time that exotic solutions, such as stable traveling breathers, have been found in a homogeneous neural field model. We attribute this interesting new physics directly to the choice of nonlinear threshold accommodation model, since linear models, of the type studied by Hansel and Sompolinsky [10], have only shown bump instabilities leading to traveling pulses. Full details of the calculations in this paper, and further explorations of parameter space, including results in two-dimensions, will be published elsewhere.

[1] H. R. Wilson and J. D. Cowan, Biophysical Journal **12**, 1 (1972).
[2] S. Amari, Biological Cybernetics **17**, 211 (1975).
[3] X. Huang, W. C. Troy, Q. Yang, H. Ma, C. R. Laing, S. J. Schiff, and J. Wu, The Journal of Neuroscience **24**, 9897 (2004).
[4] P. l Nunez, *Neocortical Dynamics and Human EEG Rhythms* (Oxford University Press, 1995).
[5] G. B. Ermentrout and J. D. Cowan, Biological cybernetics **34**, 137 (1979).
[6] P. C. Bressloff, J. D. Cowan, M. Golubitsky, P. J. Thomas, and M. Wiener, Philosophical Transactions of the Royal Society London B **40**, 299 (2001).
[7] C. R. Laing, W. C. Troy, B. Gutkin, and G. B. Ermentrout, SIAM Journal on Applied Mathematics **63**, 62 (2002).
[8] M. A. Geise, *Neural Field Theory for Motion Perception* (Kluwer Academic Publishers, 1999).
[9] K. Zhang, Journal of Neuroscience **16**, 2112 (1996).
[10] D. Hansel and H. Sompolinsky, *Methods in Neuronal Modeling, From Ions to Networks (2nd Edition)* (MIT Press, 1998), chap. Modeling Feature Selectivity in Local Cortical Circuits, pp. 499–567.
[11] S. Coombes, Biological Cybernetics **to appear** (2005).
[12] D. V. Madison and R. A. Nicoll, Journal of Physiology **345**, 319 (1984).
[13] Y. H. Liu and X. J. Wang, Journal of Computational Neuroscience pp. 25–45 (2001).
[14] A. V. Hill, Proceedings of the Royal Society of London. Series B, Biological Sciences **119**, 305 (1936).
[15] S. Coombes, G. J. Lord, and M. R. Owen, Physica D **178**, 219 (2003).
[16] S. Coombes and M. R. Owen, SIAM Journal on Applied Dynamical Systems **34**, 574 (2004).
[17] H. Sakaguchi and B. A. Malomed, Physica D **154**, 229 (2001).
[18] M. Bode, A. W. Liehr, C. P. Schenk, and H. G. Purwins, Physica D **161**, 45 (2002).
[19] P. C. Bressloff, S. E. Folias, A. Prat, and Y. X. Li, Physical Review Letters **91**, 178101 (2003).